 CMC, vol.34, no.2, pp.117-129, 2013

Effects of High Magnetic Field and Post-Annealing on the Evaporated Ni/Si (100) Thin Films

Jiaojiao Du[1], Guojian Li[1], Qiang Wang[1,2], Yongze Cao[1], Yonghui Ma[1], Jicheng He[1]

Abstract: The effects of high magnetic field and post-annealing on the structural, electrical and magnetic properties of the evaporated Ni films were investigated and compared. The in-situ application of a 6 T magnetic field during evaporation or post-annealing at 200 ^{o}C did not change the crystal structures of the films. However, the magnetic field makes the films exhibit the smallest grain size and the lowest surface roughness. Crystallinity was improved for both the 6 T films and the annealed films. This leads to the enhancement of saturation magnetization *(Ms)*. The value of *Ms* for the 0 T films was 588 emu/cm^3, while those for the 6 T films and the post-annealing films without magnetic field were 704 and 647 emu/cm^3, respectively. In addition, the 6 T films also exhibited the lowest resistivity. These results indicate that the in-situ application of high magnetic field was a much more efficient method than the post-annealing treatment in the increase of film quality and properties.

Keywords: High magnetic fields; thin films; physical vapor deposition; electrical properties; magnetic properties; annealing.

1 Introduction

Ni films play an important role in many multilayer systems, which have a lot of practical and potential applications in magnetic storage media, magnetic head components for high-density magnetic recording, semiconductor technology and giant magnetoresistance sensors [Gregg et al. (2002); Sarkar et al. (2000); Lee et al. (2002)]. In order to meet the demands of scientific and technical applications, good

[1] Key Laboratory of Electromagnetic Processing of Materials (Ministry of Education), Northeastern University, Shenyang 110819, China.

[2] Corresponding author. Key Laboratory of Electromagnetic Processing of Materials (Ministry of Education), Northeastern University, No. 3-11 Wenhua Road, Heping District, Shenyang, Liaoning Province, 110819, P. R. China.

Tel: +86-24-83681726, Fax: +86-24-83681758, E-mail address:wangq@mail.neu.edu.cn

quality and properties of Ni films are needed. Among many methods to improve the properties of materials, high magnetic field, like temperature and pressure, is one of the important thermodynamic parameters of the inner energies in materials. And it exhibits the characters of non-contact operation, enhanced Lorentz force and magnetization force. Therefore, high magnetic field is expected as a useful technology in the preparation of many functional materials. It has been given special attention in the last few decades [Wang et al. (2009); Liu et al. (2009)]. It is found that high magnetic fields can modify the structure and properties of thin films. For example, Y. W. Ma reported that the critical current density of the YBaCuO films have been improved by a high magnetic field [Ma et al. (2000)]. The remarkable perpendicular magnetic anisotropy induced by a magnetic field in Fe-Si-O film has been found in the work of H. L. Bai [Bai et al. (2001)]. High magnetic field can also affect the grain growth and surface roughness of the α'-FeN film, and enhance the magnetic softness of the films [Wang, Mitani, and Motokawa (2003)]. Superimposing an external magnetic field offers possibilities to influence the electrodeposition processes, and thus control the microstructure [Matsushima et al. (2006); Fahidy (2001)] and improve the GMR effect of the thin films [Uhlemann et al. (2003)]. Besides, Q. Wang et al [Wang et al. (2013)] found that high magnetic field has much more significant effect than that of a substrate temperature of 400 ^{o}C on enhancing the crystallinity, preferred orientation and soft magnetic properties of the NiFe film. As a ferromagnetic material, the influence of weak magnetic field on the surface morphology of Ni films has been reported early [Kaiju et al. (2009)], but the change of surface morphology is not obvious due to the low magnetic field intensity. Up to now, the effects of high magnetic fields are still unclear. On the other hand, annealing treatment can eliminate stress, improve structural characteristics and thermodynamic stability [Chang et al. (2011); Hou et al. (2003); Gupta and Mansingh (1996)], then the mechanical, electrical and magnetic properties of thin films. As two methods of increasing the film quality, little attention was paid to the comparison of the effects of in-situ application of high magnetic field and post-annealing treatment on the films. In this paper, the effects of the in-situ application of high magnetic field and post-annealing on the structural, electrical and magnetic properties of the evaporated Ni films were investigated and compared. And the relationship between the electromagnetic properties and structure evolution are also examined.

2 Experimental methods

Figure 1 shows the schematic view of the molecular beam vapor deposition (MBVD) apparatus [Wang et al. (2013); Cao et al. (2013)] in a liquid helium-free superconducting magnet system. A vacuum chamber was set in the 300 mm diameter bore of the magnet, and the direction of the generated magnetic field was set upward, which is perpendicular to the film plane. A crucible filled with the source material of 99.9999 % pure Ni particles was set into the vacuum chamber. The Si (100) substrates were situated at the position with the maximum magnetic flux density. All the Si (100) substrates were prepared by ultrasonically cleaning for 15 minutes in the acetone, alcohol and then dried by high pure Ar gas. During experiments, the temperatures of the source material and substrates are 1400 and 200 ^{o}C, respectively. The degree of vacuum in the chamber was about 8.0×10^{-5} Pa before evaporation; it reached to 2.0×10^{-4} Pa during deposition. The deposition time was fixed at 15 minutes and the deposition rate is about 1.2 nm/min. Four kinds of Ni film samples were obtained: (1) 0 T as-deposited films, no magnetic field was applied during the formation processes of the films (called 0 T film thereafter); (2) 6 T as-deposited films, a 6 T magnetic field was applied during the growth process of the films (6 T film); (3) 0 T annealed films, the 0 T films were heat treated at 200 ^{o}C for 40 minutes in vacuum (0 T annealed film); (4) 6 T annealed films, the 6 T films were heat treated same as the 0 T annealed film (6 T annealed film).

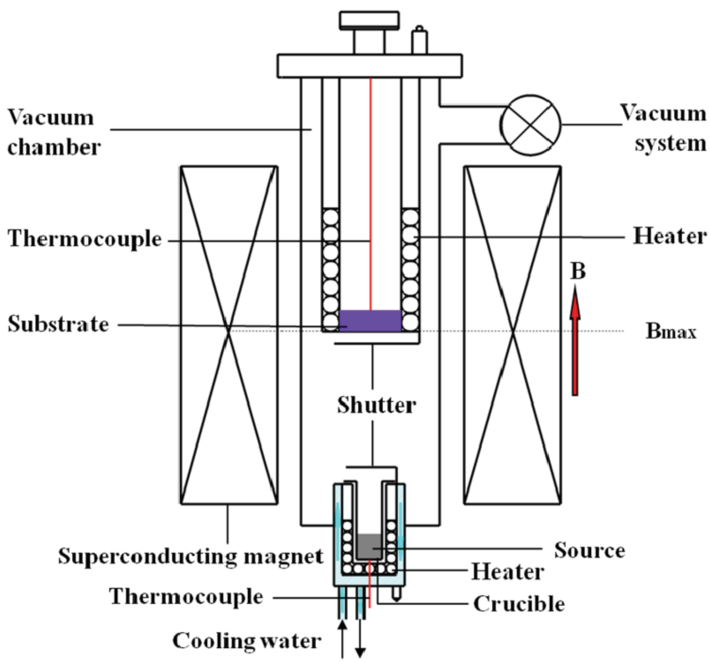

Figure 1: Schematic view of the molecular beam vapor deposition apparatus in a superconducting magnet.

Film thicknesses were measured by using a surface profiler (alpha-step IQ) with a vertical resolution of 0.75 nm. All the thicknesses of Ni films were around 18 nm. Structural properties were studied by using a grazing incidence of DMAX 2400 X-ray diffractometer (XRD), which works in the θ-2θ mode with a monochromatic Cu Kα1 radiation (λ=0.154056 nm). Scanning range is from 40 to 100^o with 0.04^o increments and scanning rate is 1°/min. A Nanoscope *IV* atomic force microscope (AFM) was used to study the surface morphology and roughness. The magnetic parameters were deduced from a lakeshore 7407 vibrating sample magnetometer (VSM). The electrical resistivity was obtained from the sheet resistance which was measured by the four-point method (RTS-9).

3 Results and discussion

3.1 X-ray diffraction results

Figure 2 shows the XRD patterns of the Ni films under different conditions, at the same time, the peaks of the Si substrate are also shown. Clearly, for all the films, the substrate peak appears at about 51.6°. Ni fcc (111) and (220) peaks appear for all the films. Furthermore, fcc (311) peak exists for the 6 T film and the post-annealing films. No other phases such as nickel silicate or nickel oxide were seen in the XRD results. This indicates that the film is polycrystalline fcc structure, without any impurity. And the effects of high magnetic field and post-annealing did not change the crystal structures of the films. In addition, the XRD peak area ratio, *A* (111)/*A* (220) was used to consider the preferred orientation and film crystallinity, as shown in Figure 3. The ratios for the 6 T, post-annealing films are larger than that of the 0 T film. It can also be seen that the ratios of the film with a 6 T magnetic field are more significant than that of the 0 T annealing film. That is say, the diffraction peak of (111) shows stronger preferred orientation than that of (220) for the 6 T film and the 6 T annealed film than that of 0 T annealed film. Furthermore, both the high magnetic field and post-annealing can increase the crytallinity, but the effect of high magnetic field is much more efficient than the heat treatment.

The grain sizes were calculated by using Scherrer equation [Ghebouli et al. (2007)], which is given by: $D = K\lambda \big/ \beta \cos\theta$, where D is the grain size with a particular orientation, K is a constant close to 1, λ is the X-ray wavelength (λ=0.154056 nm), β is the width at half height of the corresponding (111) peak, respectively. The average grain size is shown in Table 1. Grain size of the 6 T films (6.9 nm) was obviously smaller than that of the 0 T films (9.7 nm). This means that high magnetic field has great effect on the grain refinement. For the 0 T annealed films, the grain size is 12.1 nm, which was increased by 20 % in comparison to the 0 T films. Larger grains of the 6 T annealed films compared to the 6 T films were

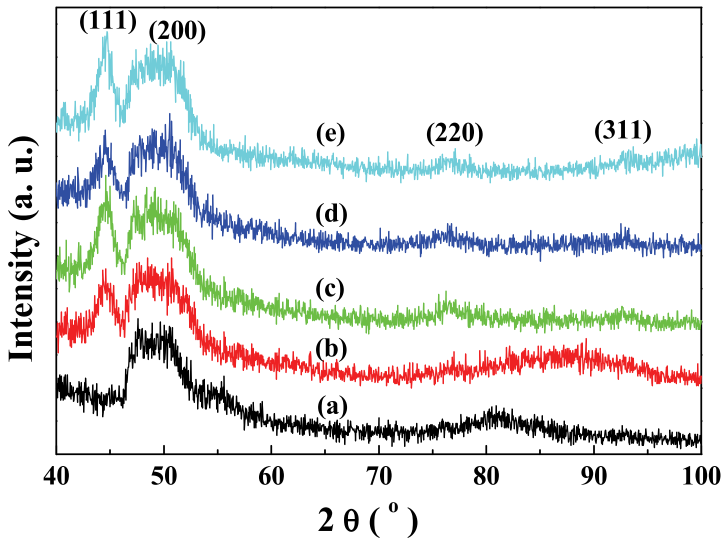

Figure 2: X-ray diffraction patterns of (a) Si (100) substrate; (b) 0 T film; (c) 6 T film; (d) 0 T annealed film; (e) 6 T annealed film.

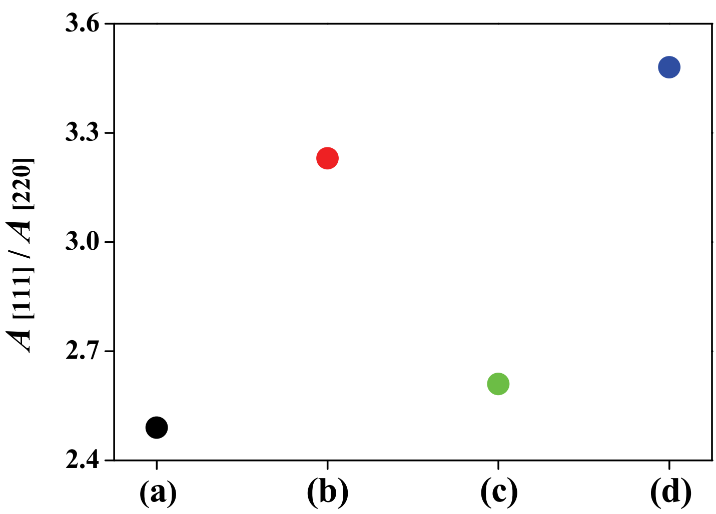

Figure 3: The area ratio *A* (111)/*A* (220) for the four films (a) 0 T film; (b) 6 T film; (c) 0 T annealed film; (d) 6 T annealed film.

also observed. In addition, the grain size of the 6 T annealed film (11.9 nm) is still smaller than that of the 0 T annealed film (12.1 nm).

Table 1: Average grain size (D_1) calculated from XRD, area ratio A (111)/A (220), for the Ni films under different preparation conditions.

Samples	Grain size D_1(nm)	Area ratio A (111)/A (220)
0 T films	9.7	2.49
6 T films	6.9	3.23
0 T annealed films	12.1	2.61
6 T annealed films	11.9	3.48

3.2 Surface morphology and roughness

Figure 4 shows the typical AFM images and the corresponding histograms of particle size. All the Ni films consist of small crystalline nanoparticles. The total number of particles of the shown area in Fig. 4, and the surface roughness of each film are summarized in Table 2. The roughness of the films is the average value of four typical areas of $1.5\mu m \times 1.5\mu m$ for each film. We choose 200 typical particles from the scan area of Fig. 4, and obtain the average particle size (shown in Fig. 4 and Table 2). In order to demonstrate the homogeneity of the layers, the particle size distribution is assumed to be a Gaussian fit, and the standard deviation σ is also calculated for each film. It is clearly visible that the particles of the 6 T films were obviously refined by the high magnetic field (shown in Fig. 4 (a) and (b)). Moreover, the 6 T films possess more homogeneous, smoother surface and narrower particle distribution than that of the 0 T films. In addition, the particle sizes of the 0 T annealed and 6 T annealed films are larger than that of the corresponding as-deposited counterparts. The roughness of films develops due to the large particle size [Gupta and Mansingh (1996); Rafique et al. (2008); Yi et al. (2007)]. As a result, the particle size and roughness of the 6 T annealed films are less than the 0 T annealed films. The particle size of different films is about 26-47 nm, which is much larger than the grain size as obtained from XRD, implying that these particles were agglomerates of small grains [Yi et al. (2004)]. From above we can see that the 6 T film possesses the smoothest surface and smallest particles among the four kinds of films. And the smallest standard deviations show the homogeneity in grain structure for the 6 T film. This is further indicated that the effect of high magnetic field is more significant than the annealing treatment on reducing surface roughness and enhancing the uniformity of layers. Similar results were also found in other samples.

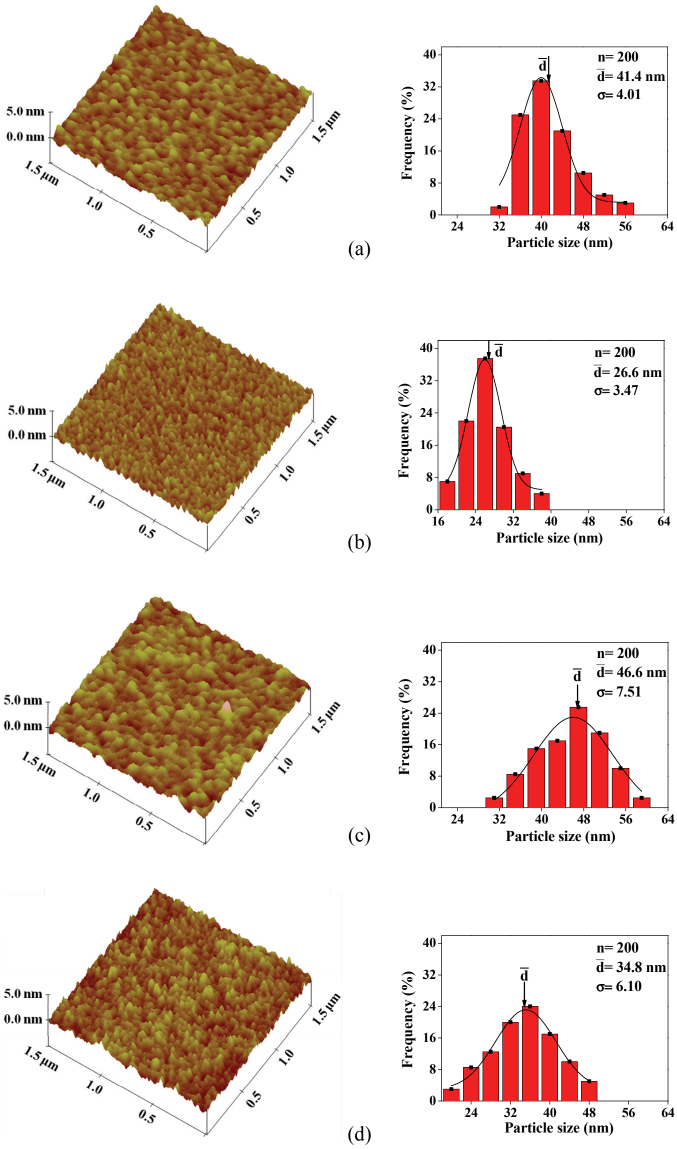

Figure 4: Typical AFM images of the Ni films (left panel) and respective histograms of particle size distributions (right panel). The black line in the histograms is the Gaussian fit. Note that the statistical particle number n, the mean particle size d and the standard deviation σ are shown in each histogram (a) 0 T film; (b) 6 T film; (c) 0 T annealed film; (d) 6 T annealed film.

Table 2: Numbers of particles of the shown area in AFM image of Fig. 4 (N), average particle size (D_2) obtained from AFM, surface roughness (R_q), electrical resistivity (ρ), for the Ni films under different preparation conditions.

Samples	Number of particles N	Particle size D_2 (nm)	Surface roughness R_q (nm)	Electrical resistivity $\rho(\mu\Omega\cdot cm)$
0 T	360	41.4	0.26	58.9
6 T	724	26.6	0.24	33.8
0 T annealed	318	46.6	0.33	46.8
6 T annealed	534	34.8	0.32	35.1

3.3 Magnetic properties

It is well known that the microstructures of materials dominate their properties. The magnetic hysteresis loops ($M-H$ loop) of the 0 T film at room temperature with the applied fields parallel and perpendicular to the film plane are shown in Figure 5 (a). With the applied field parallel to the film plane, the $M-H$ loop is relatively square with large remanence and low coercivity, characteristics of the magnetic easy axis [Sun, Chien, and Searson (2004)]. For the other three films, the magnetic easy axis is also parallel to the film plane (the $M-H$ loops with H perpendicular to the film plane are not shown here). Figure 5 (b) exhibits the $M-H$ loops for the four kinds of films when H is parallel to the film plane. The saturation magnetization (Ms) of the 6 T, 0 T annealed, and 6 T annealed films are 704, 647, and 788 emu/cm^3, respectively, which are all larger than that of the 0 T films (588 emu/cm^3). The Ms of all the samples is higher than the value of the corresponding bulk Ni (521.27 emu/cm^3) [Ye, Chen, and Zheng (2008)]. Good crystalline quality and grain coupling can lead to the increase of magnetic properties [Ye, Chen, and Zheng (2008); Nam et al. (2001); Chen et al. (2000); Barrero, Vandenberghe, and Grave (1999); Ma et al. (2006)]. In this study, the 6 T film and annealed films possess good crystallinity than the 0 T film and also the small grains of uniform size, the smooth surface, these may cause the increase of Ms of the 6 T films. For the 0 and 6 T annealed films, the grain size is increased. However, it is also recognized that the larger the grain, the lower the density of the grain boundaries. Thus the exchange coupling between grains is enhanced [Ma et al. (2006)]. This good grain coupling leads to the improvement of Ms. It is the reason why the Ms of the annealed sample is larger than that without annealing. In one word, applying a magnetic field induces a 20 % increase of Ms comparing to that of the 0 T films, which is a much more efficient way to improve the Ms than the annealing treatment (only 10 % improvement on *Ms*). However, magnetic field and annealing can hardly change the coercive field, remaining a value of the order of 24 Oe for all the four films.

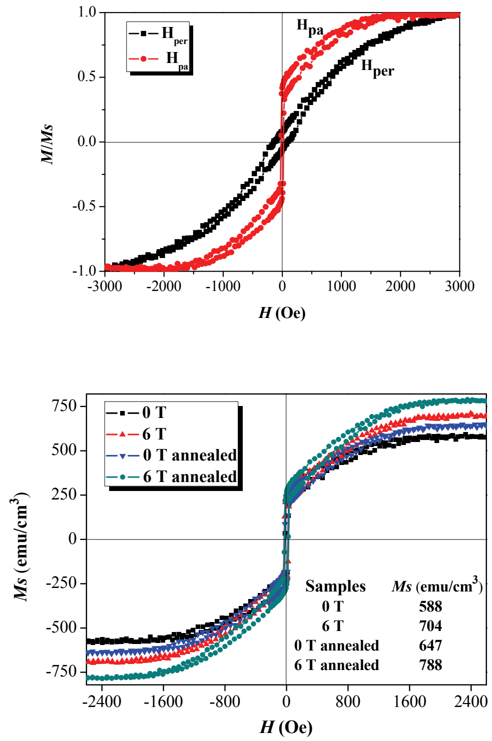

(a)

(b)

Figure 5: Room temperature $M - H$ curves for: (a) the 0 T film with the applied magnetic fields parallel and perpendicular to the film plane; (b) the four films when the applied magnetic field is parallel to the plane, the bottom right inset shows the values of magnetic properties of the four samples.

3.4 Electrical properties

The sheet resistance (R) is defined as $R = \rho/t$, where ρ is the electrical resistivity and t is the film thickness; R is measured in Ohms/square $(\Omega/)$. In this study, the sheet resistances have been measured for all samples by the four point probe method [Mebarki et al. (2011)]. These data of four samples are listed in Table 2. It is clear that the highest resistivity (ρ = 58.9 $\mu\Omega$ cm) appears in the 0 T film. The resistivity of the 6 T film is found to be 33.8 $\mu\Omega$ cm, which is a decrease nearly by 43 % comparing to that of the 0 T film. It can be concluded that a 6 T magnetic field can greatly reduce the resistivity of the Ni film. The enhancement in crystallinity of the film resulted in the low point defect density [Xu, Shao, and Jin (2009)]. Therefore, the 0 T film possesses the highest value of resistivity due to the poor crystallinity. It is known that the resistivity depends on the product of the charge carrier density and the carrier mobility [Xu, Shao, and Jin (2009)]. In general, the carrier mobility is inversely proportional to film roughness and the carrier concentration is proportional to grain size [Shin and Yoon (1997)]. Therefore, for the 6 T film, the perfect crystallinity and the increase of the charge carrier mobility due to the smooth surface lead to the decrease of resistivity. The resistivity of the 0 T annealed film is a little lower (46.8 $\mu\Omega$ cm) than that of the 0 T film. The resistivity of the 0 T annealed film can be relatively well described with the Mayadas-Sondheimer model [Mayadas and Shatzkes (1970)]. Grain boundary amounts decrease owing to the increase of particle size in the 0 T annealed film. Thus the resistivity of the 0 T annealed film decreased. However, the resistivity of the 6 T annealed film (35.1 $\mu\Omega$ cm) is a little higher than that of the 6 T film. Comparing the effects of magnetic field to that of annealing method, the magnetic field exhibits larger controlling effect on the film resistivity.

4 Conclusions

This paper has demonstrated the effects of high magnetic field and post-annealing on the structure, electrical and magnetic properties of the Ni films prepared by molecular beam vapor deposition method. The conclusions were shown as follows: Both a 6 T magnetic field and post annealing can promote the crystallinity of Ni films. Furthermore, the influence of high magnetic field is more significant. The 6 T magnetic field can make the homogeneity increase but the surface roughness and grain size decrease of the film surface. Both annealing treatment and a 6 T magnetic field can improve the saturation magnetization due to the good crystallinity, and applying a 6 T magnetic field is a much more efficient way to increase Ms. However, there are no obvious differences in the coercivity. It is found that high magnetic field plays an important role in the decrease of the resistivity of the Ni film.

Acknowledgments

This work was financially supported by the National Natural Science Foundation of China (Grant Nos. 51061130557, 51101032, 51101034), the Fundamental Research Funds for the Central Universities (Grant Nos. N120609001, N110408006 and N120509001).

References

Gregg, J. F.; Petej, I.; Jouguelet, E.; Dennis, C. (2002): Spin electronics-a review. *J. Phys. D: Appl. Phys.,* vol. 35, pp. R121-R155.

Sarkar, D. K.; Falke, M.; Giesler, H.; Teichert, S.; Beddies, G.; Hinneberg, H. J. (2000): Role of buried ultra thin interlayer silicide on the growth of Ni film on Si (100) substrate. *Appl. Phys. A,* vol. 70, pp. 681-684.

Lee, P. S.; Pey, K. L.; Mangelinck, D.; Ding, J.; Chi, D. Z.; Osipowicz, T.; Dai, J. Y.; Chan, L. (2002): Effect of ion implantation on layer inversion of Ni silicided poly-Si. *J. Electrochem. Soc.,* vol. 149, pp. G505-G509.

Wang, Q.; Lou, C. S.; Liu, T.; Wei, N.; Wang, C. J.; He, J. C. (2009): Fabrication of MnBi/Bi composite using dilute master alloy solidification under high magnetic field gradients. *J. Phys. D: Appl. Phys.,* vol. 42, pp. 025001 (1-5).

Liu, T.; Wang, Q.; Gao, A.; Zhang, C.; Li, D. G.; He, J. C. (2009): Crystal orientation and grain alignment in a hypoeutectic Mn-Sb alloy under high magnetic field conditions. *J. Alloy Compd.,* vol. 481, pp. 755-760.

Ma, Y. W.; Watanabe, K.; Awaji, S.; Motokawa, M. (2000): J_c enhancement of $YBa_2Cu_3O_7$ films on polycrystalline silver substrates by metalorganic chemical vapor deposition in high magnetic fields. *Appl. Phys. Lett.,* vol. 77, pp. 3633-3635.

Bai, H. L.; Mitani, S.; Wang, Z. J.; Fujimori, H.; Motokawa, M. (2001): Anomalous RF sputtering in a high magnetic field: the effect of high magnetic fields on the growth of Fe–Si–O films. *Thin solid films,* vol. 389, pp. 51-55.

Wang, H. Y.; Mitani, S.; Motokawa, M. (2003): Effect of high magnetic fields on the morphology of soft magnetic $\alpha\prime$-FeN films. *J. Appl. Phys.,* vol. 93, pp. 9145-9150.

Matsushima, H.; Fukunaka, Y.; Ito, Y.; Bund, A.; Plieth, W. (2006): Anomalous scaling of iron thin film electrodeposited in a magnetic field. *J. Electroanal. Chem.,* vol. 587, pp. 93-98.

Fahidy, T. Z. (2001): Characteristics of surfaces produced via magnetoelectrolytic deposition. *Prog. Surf. Sci.,* vol. 68, pp. 155-188.

Uhlemann, M.; Gebert, A.; Herrich, M.; Krause, A.; Cziraki, A.; Schultz, L. (2003): Electrochemical deposition and modification of Cu/Co–Cu multilayer. *Electrochim. Acta,* vol. 48, pp. 3005-3011.

Wang, Q.; Cao, Y. Z.; Li, G. J.; Wang, K.; Du, J. J.; He, J. C. (2013): Improving magnetic properties of molecular-beam-vapor-deposited Ni45Fe55 nanocrystalline films by in situ high magnetic field application. *Sci. Adv. Mater.,* vol. 5, pp. 1-6.

Kaiju, H.; Ono, A.; Kawaguchi, N.; Kondo, K.; Ishibashi, A.; Won, J.; Hi-

rata, A.; Ishimaru, M.; Hirotsu, Y. (2009): Ni thin films vacuum-evaporated on polyethylene naphthalate substrates with and without the application of magnetic field. *Appl. Surf. Sci.,* vol. 255, pp. 3706-3712.

Chang, W. C.; Qi, X. D.; Kuo, J. C.; Lee, S. C.; Ng, S. K.; Chen, D. (2011): Post-deposition annealing control of phase and texture for the sputtered MoO_3 films. *CrystEngComm,* vol. 13, pp. 5125-5132.

Hou, Y. Q.; Zhuang, D. M.; Zhang, G.; Zhao, M.; Wu, M. S. (2003): Influence of annealing temperature on the properties of titanium oxide thin film. *Appl. Surf. Sci.,* vol. 218, pp. 97-105.

Gupta, V.; Mansingh, A. (1996): Influence of postdeposition annealing on the structural and optical properties of sputtered zinc oxide film. *J. Appl. Phys.,* vol. 80, pp. 1063-1073.

Cao, Y. Z.; Wang, Q.; Li, G. J.; Du, J. J.; Wu, C.; He, J. C. (2013): Effects of high magnetic field on the structure evolution, magnetic and electrical properties of the molecular beam vapor deposited FexNi1-x ($0.3 \leq x < 0.8$) thin films. *J. Magn. Magn. Mater.,* vol. 332, pp. 38-43.

Ghebouli, B.; Cherif, S. M.; Layadi, A.; Helifa, B.; Boudissa, M. (2007): Structural and magnetic properties of evaporated Fe thin films on Si (111), Si (100) and glass substrates. *J. Magn. Magn. Mater.,* vol. 312, pp. 194-199.

Rafique, M. S.; Khaleeq-ur-Rahman, M.; Rehman, S.; Anjum, S.; Anwar, M. S.; Bhatti, K. A.; Saeed, S.; Awan, M. S. (2008): Effect of external magnetic field on the deposition of $BaFe_{12}O_{19}$. *Vacuum,* vol. 82, pp. 1233-1237.

Yi, J. P.; Li, X. P.; Ding, J.; Seet, H. L. (2007): Study of the grain size, particle size and roughness of substrate in relation to the magnetic properties of electroplated permalloy. *J. Alloy Compd.,* vol. 428, pp. 230-236.

Yi, J. B.; Zhou, Y. Z.; Ding, J.; Chow, G. M.; Dong, Z. L.; White, T. J. (2004): An investigation of structure, magnetic properties and magnetoresistance of Ni films prepared by sputtering. *J. Magn. Magn. Mater.,* vol. 284, pp. 303-311.

Sun, L.; Chien, C. L.; Searson, P. C. (2004): Fabrication of nanoporous nickel by electrochemical dealloying. *Chem. Mater.,* vol. 16, pp. 3125-3129.

Ye, J.; Chen, Q. W.; Zheng, Y. Q. (2008): Magnetic properties of nickel film formed under magnetic fields. *J. Phys. D: Appl. Phys.,* vol. 41, pp. 205011 (1-5).

Nam, B. C.; Kim, W. S.; Choi, H. S.; Kim, J. C.; Hur, N. H.; Kim, I. S.; Park, Y. K. (2001): Effect of oxygen annealing on the magnetoresistance in La0.7Ca0.3MnO3 epitaxial films. *J. Phys. D: Appl. Phys.,* vol. 34, pp. 54-59.

Chen, M. S.; Shen, Z. X.; Liu, X. Y.; Wang, J. (2000): Raman and magnetization studies of barium ferrite powder prepared by water-in-oil microemulsion. *J. Mater.*

Res., vol. 15, pp. 483-487.

Barrero, C. A.; Vandenberghe, R. E.; Grave, E. De. (1999): The effect of Al-content and crystallinity on the magnetic properties of goethites. *Hyperfine Interactions,* vol. 122, pp. 39-46.

Ma, Y. W.; Xu, A. X.; Li, X. H.; Zhang, X. P.; Guilloux-Viry, M.; Pena, O.; Awaji, S.; Watanabe, K. (2006): Improved properties of epitaxial $YNi_xMn_{1-x}O_3$ films by annealing under high magnetic fields. *Appl. Phys. Lett.,* vol. 89, pp. 152505 (1-3).

Mebarki, M.; Layadi, A.; Guittoum, A.; Benabbas, A.; Ghebouli, B.; Saad, M.; Menni, N. (2011): Structural and electrical properties of evaporated Fe thin films. *Appl. Surf. Sci.,* vol. 257, pp. 7025-7029.

Xu, J.; Shao, T. M.; Jin, G. (2009): Effect of processing conditions on microstructure and electrical characteristics of Ni thin film. *Vacuum,* vol. 84, pp. 478-482.

Shin, W. C.; Yoon, S. G. (1997): Characterization of RuO_2 thin films prepared by hot-wall metallorganic chemical vapor deposition. *J. Electrochem. Soc.,* vol. 144, pp. 1055-1060.

Mayadas, A. F.; Shatzkes, M. (1970): Electrical-resistivity model for polycrystalline films: the case of arbitrary reflection at external surfaces. *Phy. Rev. B,* vol. 1, pp. 1382-1389.